Bull. Mater. Sci., Vol. 40, No. 2, April 2017, pp. 329–333. © Indian Academy of Sciences.
DOI 10.1007/s12034-017-1377-1

Visible-light-induced hydrogen evolution reaction with WS_xSe_{2-x}

UTTAM GUPTA* **and DEEPA S NARANG**
Chemistry and Physics of Materials Unit, New Chemistry Unit, International Centre for Materials Science and Sheikh Saqr Laboratory, Jawaharlal Nehru Centre for Advanced Scientific Research, Jakkur P.O., Bangalore 560 064, India

MS received 4 July 2016; accepted 5 July 2016

Abstract. **WS_2 is a promising catalyst for the hydrogen evolution reaction. We have explored photocatalytic properties of ternary sulphoselenides of tungsten (WS_xSe_{2-x}) by the dye-sensitized hydrogen evolution. WS_xSe_{2-x} solid solutions are found to exhibit high activity reaching 2339 μmol h^{-1} g^{-1} for WSSe, which is three times higher than that of WS_2 alone (866 μmol h^{-1} g^{-1}). The turnover frequency is also high (0.7 h^{-1}). Such synergistic effect of selenium substitution in WS_2 is noteworthy.**

Keywords. **Layered chalcogenides; photochemical hydrogen evolution, tungsten sulphoselenides.**

1. Introduction

Transition metal dichalcogenides (TMDs) have emerged as an important class of materials with unique properties [1–4]. They have layered sandwiched X–M–X units (M = metal and X = chalcogenides) with strong in-plane bonding and weak out-of-plane van der Waals interaction between layers. Among the layered TMDs, MoS_2 and $MoSe_2$ have attracted the significant attention in the last few years due to their properties related to transistors [5,6], catalysis [8–10] and gas sensors [10]. They are also useful for hydrogen evolution catalysis. Theoretical and experimental studies indicate that the (0001) planes are catalytically inert, while (10–10) planes are catalytically active due to the low Gibbs free energy for hydrogen evolution reaction (HER) [11,12]. Various strategies have been employed to improve the HER either by creating much active edge sites [13–17] or by chemical modification with Fe, Co, Ni and Re [17,18]. The metastable 1T-phase exhibits improved catalytic activity for HER. Ternary composites of TMDs $MoS_{2(1-x)}Se_{2x}$ [19,20] and MoS_xCl_y [21] are reported to show improved performance compared with binary compounds in electrochemical HER. We have synthesized ternary WS_xSe_{2-x} ($x = 0.0$, 0.50, 1.0, 1.5, 2.0) and examined their photocatalytic HER activity. Interestingly, we found synergistic effect wherein the ternary sulphoselenides are superior catalysts compared with the binary compounds.

2. Experimental

Tungsten sulphoselenides, WS_xSe_{2-x} ($x = 0$, 0.5, 1, 1.5, 2.0), were synthesized by the solid-state reaction of a stoichiometric mixture of tungsten (W) (99.99+% Sigma Aldrich) with sulphur (S) (99.99% Sigma Aldrich) and selenium (Se) (Sigma Aldrich) of 99.99% purity. The mixture was loaded in a high-quality quartz tube (12 mm OD, 10 mm ID, 22 cm length) and sealed under vacuum at 10^{-6} Torr. The sealed tube was introduced into a furnace and slowly heated to 850°C for over 15 h. The quartz tube was kept at the same temperature for 48 h and cooled slowly to room temperature. The products were also characterized by X-ray diffraction (XRD) using a Bruker D8 Advance X-ray diffractometer (Cu K_α; $\lambda = 1.54$ Å). Raman spectra were recorded with 514 nm Argon laser using a Jobin-Yvon Labram HR spectrometer. The scanning electron microscope (SEM) images were taken using a NOVA nano-FESEM. The BET surface area measurement was calculated by N_2 adsorption using a Quantachrome Autosorb instrument at 77 K.

WS_xSe_{2-x} samples ($x = 0.0$, 0.50, 1.0, 1.5, 2.0) were dispersed in a solution of triethanolamine (TEAO, 15% v/v) in water. To this dispersion 0.014 mM of Eosin Y dye was added and the system purged with N_2. Hydrogen evolution studies were carried out with a 100 W halogen lamp under constant stirring. The evolved gas was analysed over a period using a Perkin Elmer 580 C Clarus GC-TCD.

Turnover frequency (TOF) was calculated using the equation

$$\mathrm{TOF}\left(\mathrm{h}^{-1}\right) = \frac{\text{Activity of the catalyst}}{\text{Moles of the catalyst used}} \qquad (1)$$

3. Results and discussion

XRD patterns confirm the hexagonal 2H-structure for all the WS_xSe_{2-x} compositions, with a prominent peak due to the (002) reflection (figure 1a). There is a shift in the reflection to lower angles with increasing substitution of sulphur by selenium (figure 1b). Typical SEM images shown in figure 2a and b show the flake-like morphology of the samples. The lateral size of the flakes is ∼10 μm, while the thickness is

---

*Author for correspondence (uttamgupta@jncasr.ac.in)

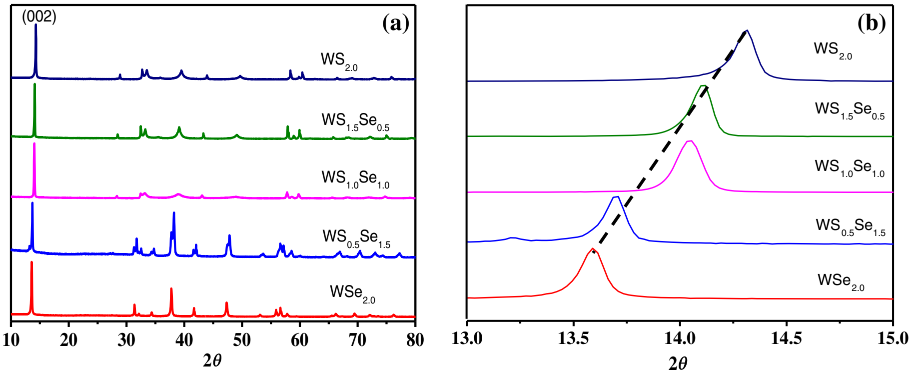

Figure 1. (a) X-ray diffraction (XRD) and **(b)** shift in the (002) peak in XRD of bulk WS_xSe_{2-x} $(x = 0, 0.5, 1.0, 1.5, 2.0)$.

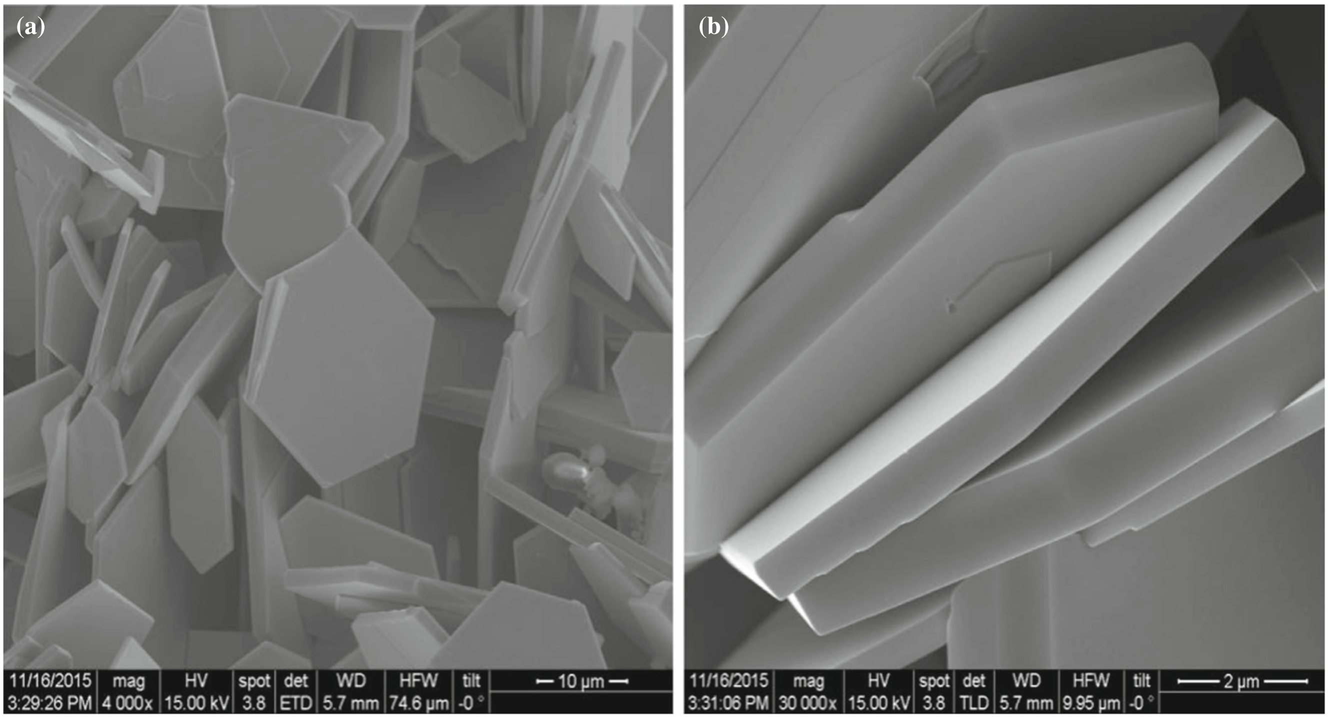

Figure 2. Typical scanning electron microscope image of the **(a)** horizontal and **(b)** cross-sectional view of the particles of the compound. The size and thickness of the particles are on an average ∼10 and ∼1 µm, respectively.

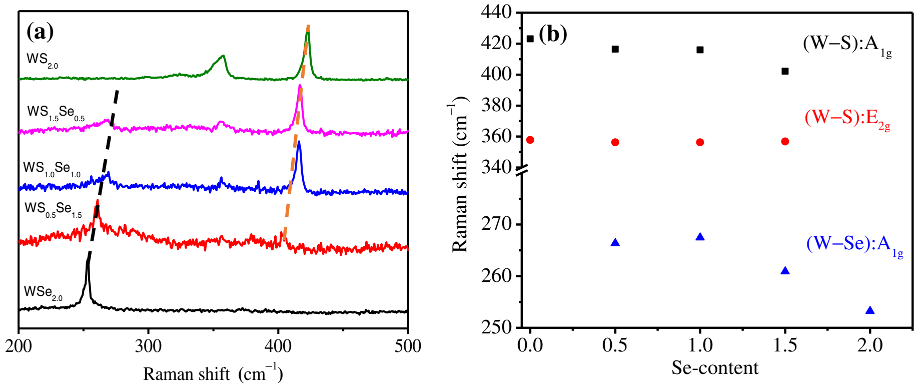

Figure 3. **(a)** Raman spectra and **(b)** shift in the W–Se A_{1g}, W–S E_{2g} and W–S A_{1g} bands in Raman of bulk WS_xSe_{2-x} $(x = 0, 0.5, 1.0, 1.5, 2.0)$.

<1 μm. The composition of the samples was ascertained by energy-dispersive spectra (EDS).

Raman spectra, recorded using a 514 nm unpolarized Ar laser with backscattered geometry (figure 3a), show two prominent first-order modes E_{2g} and A_{1g} modes at 358 and 423 cm^{-1}, respectively. The other first-order mode due to the longitudinal acoustic mode appears as a small hump at 177 cm^{-1}. WSe_2 shows a prominent band at 253 cm^{-1} due to the out-of-plane second-order mode of the longitudinal 2LA mode at 251 cm^{-1}, which overlaps with the E^1_{2g} mode [22–24]. With the increase in Se content of WS_xSe_{2-x}, a red-shift is observed in the A_{1g} band but the E_{2g} band shows no significant change (figure 3b). Disorder in the crystallites induces some broadening of the Raman peaks [25,26].

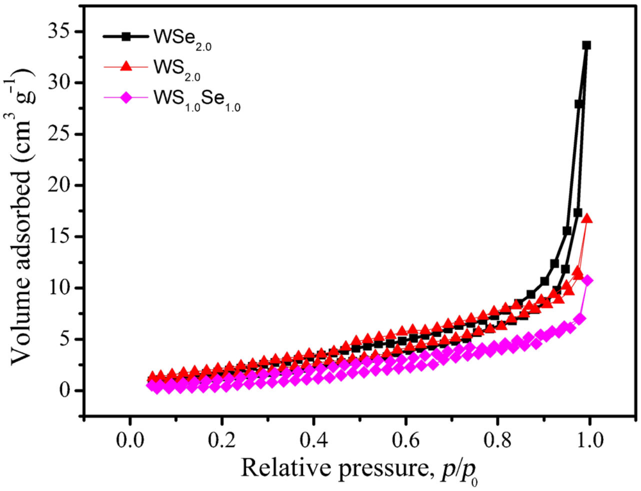

Figure 4. The BET N_2 adsorption isotherm of WS_2, WSe_2 and $WS_{1.0}Se_{1.0}$.

BET surface areas of WS_xSe_{2-x} composition are in the 4–6 m^2 g^{-1} range with type-III isotherm (figure 4). Catalytic activities of these compounds would, therefore, be independent of the surface area. Dye-sensitized photochemical reaction was performed using TEAO as a sacrificial agent with Eosin Y as a photosensitizer. Eosin Y, on the absorption of photon, undergoes a transition from a singlet to a lowest lying triplet state (EY^{3*}) through intersystem crossing. EY^{3*} takes up an electron from TEAO and gets converted to EY^-. EY^- is highly reactive and transfers the electron to the hydrogen evolution site [8,9]. The activities in the first 3 h of WS_2 and WSe_2 were 691 and 1732 μmol h^{-1} g^{-1} of hydrogen with TOF of 0.17 and 0.59 h^{-1}, respectively. The activities of the solid solutions of $WS_{1.5}Se_{0.5}$, $WS_{1.0}Se_{1.0}$ and $WS_{0.5}Se_{1.5}$ compounds were 880, 1567 and 1202 μmol h^{-1} g^{-1} with TOF of 0.24, 0.36 and 0.38 h^{-1}, respectively (figure 5a). The activity of the catalyst increases with further addition of the dye, where activities of WS_2, $WS_{1.5}Se_{0.5}$, $WS_{1.0}Se_{1.0}$, $WSe_{0.5}S_{1.5}$ and WSe_2 are 866, 955, 2339, 1491 and 1480 μmol h^{-1} g^{-1} with TOF of 0.21, 0.26, 0.70, 0.47 and 0.51, respectively. The activity of bulk WSe_2 (1732 μmol h^{-1} g^{-1}) is slightly higher than that of $WS_{1.0}Se_{1.0}$ (1567 μmol h^{-1} g^{-1}) in the first 3 h but decreases after 3 h. The activity of WSSe is 2339 μmol h^{-1} g^{-1}, whereas it is 1480 μmol h^{-1} g^{-1} for WSe_2 (figure 5a and b). However, we observe a

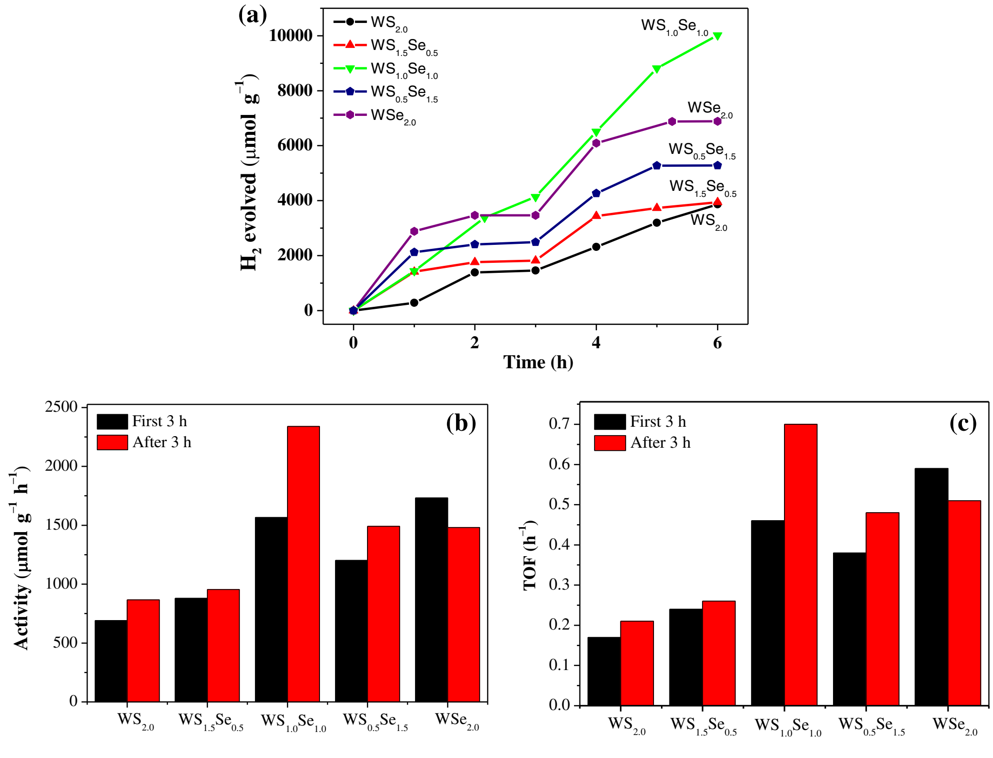

Figure 5. Comparative study of hydrogen evolution with WS_xSe_{2-x}(x = 0, 0.5, 1.0, 1.5, 2) **(a)** over a period of time. The bar graphs compare **(b)** the activity and **(c)** TOF.

Table 1. Comparison of hydrogen evolution with bulk WS_xSe_{2-x}.

Compound	Activity (μmol h^{-1} g^{-1})	TOF (h^{-1})
$WS_{2.0}$	866	0.21
$WS_{1.5}Se_{0.5}$	955	0.26
$WS_{1.0}Se_{1.0}$	2339	0.70
$WS_{0.5}Se_{1.5}$	1491	0.47
$WSe_{2.0}$	1480	0.51

The activity and TOF values are after 3 h and further addition of dye.

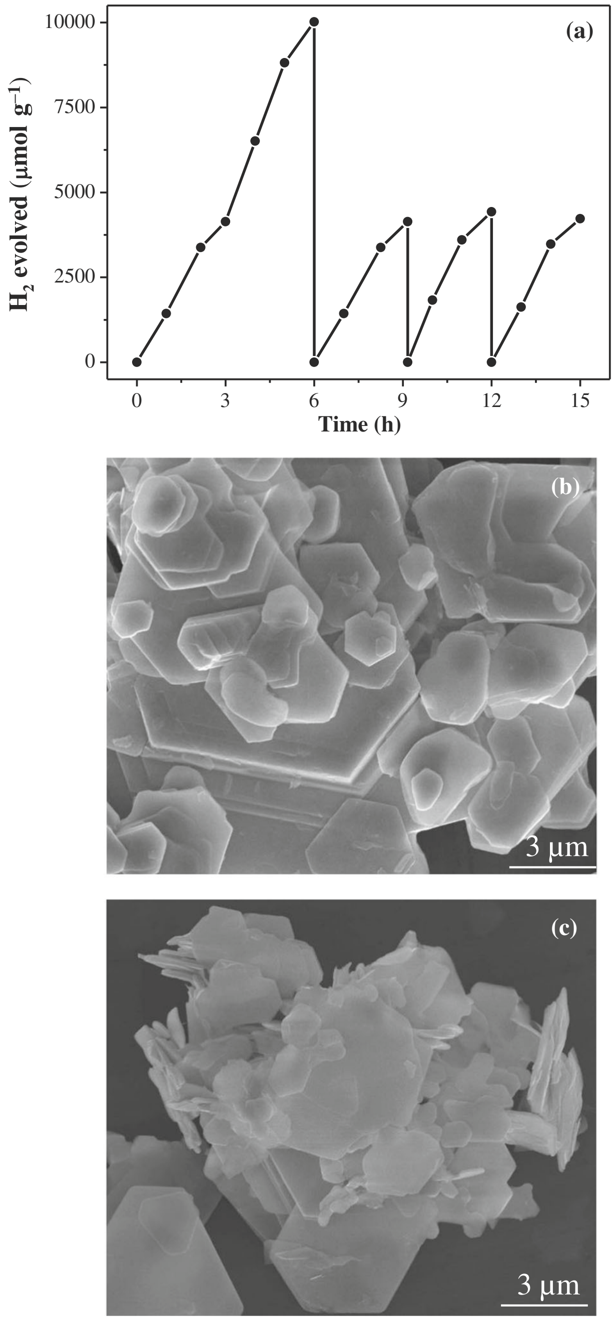

Figure 6. The cyclic study of photocatalytic HER on $WS_{1.0}Se_{1.0}$. The SEM images **(a)** before and **(b)** after photocatalytic HER. The morphology is unchanged after the cycling studies.

decrease in the activity of WSe_2 on further addition of dye after 3 h, suggesting that it will not be an optimal choice as a long-term catalyst. Figure 5b and c and table 1 show comparative activities and TOF of these compounds, where we can clearly see the enhanced hydrogen evolution (2–3 times higher than that from WS_2) of the solid solution with a maximum at $WS_{1.0}Se_{1.0}$, which indicates synergistic effect. The introduction of selenium into WS_2 induces a slight distortion in the structure because of the larger radius of selenium as compared with S. This could facilitate bond breaking of the molecules adsorbed on the basal plane. The basal plane with unsaturated bonds provides favourable hydrogen binding energy from the tensile regions on the surface, with active sites mainly located in the basal plane [27,28]. Previous studies of alloys of Se, S and W suggest that distortions can make the surface active and thus provide more sites for hydrogen samples compared with the binary compounds [29–31]. Hydrogen evolution was stable for 5 cycles (over a period of 15 h) as shown in figure 6a. There was no change in the sample before and after the HER (figure 6b and c).

4. Conclusions

In summary, we have synthesized layered binary solid solution of WS_2 and WSe_2 by a sealed tube reaction and characterized it appropriately. Visible-light dye-induced photocatalytic study indicates higher hydrogen evolution studied in WS_xSe_{2-x} compared with the parent binary counterparts, showing maximum yield at WSSe. The result suggests a synergistic effect of substitution of Se in the HER activity of the solid solutions.

Highlights

(1) Bulk synthesis of ternary transition metal dichalcogenides, tungsten sulphoselenide
(2) Composition-dependent X-ray diffraction patterns of sulphoselenide of tungsten
(3) Composition-dependent Raman
(4) Photochemical hydrogen evolution
(5) Role of anion substitution in hydrogen evolution of tungsten sulphoselenides.

Acknowledgements

We would like to sincerely thank Prof C N R Rao, FRS, for his constant guidance, support and encouragement. We would also like to thank Sonu K P for BET measurements. DSN is thankful to DST, Government of India, for the award of the post-doctoral fellowship for nanoscience and nanotechnology.

References

[1] Chhowalla M, Shin H S, Eda G, Li L, Loh K P and Zhang H 2013 *Nat. Chem.* **5** 63

[2] Rao C N R, Maitra U and Waghmare U V 2014 *Chem. Phys. Lett.* **609** 172

[3] Rao C N R, Matte H S S R and Maitra U 2013 *Angew. Chem. Int. Ed.* **52** 13162

[4] Rao C N R and Maitra U 2015 *Annu. Rev. Mater. Res.* **45** 29

[5] Radisavljevic B, Radenovic A, Brivio J, Giacometti V and Kis A 2011 *Nat. Nanotechnol.* **6** 147

[6] Late D J, Liu B, Matte H S S R, Dravid V P and Rao C N R 2012 *ACS Nano* **6** 5635

[7] Chen J, Wu X-J, Yin L, Li B, Hong X, Fan Z, Chen B, Xue C and Zhang H 2015 *Angew. Chem. Int. Ed.* **127** 1226

[8] Maitra U, Gupta U, De M, Datta R, Govindaraj A and Rao C N R 2013 *Angew. Chem. Int. Ed.* **52** 13057

[9] Gupta U, Naidu B S, Maitra U, Singh A, Shirodkar S N, Waghmare U V and Rao C N R 2014 *APL Mater.* **2** 092802

[10] Late D J, Huang Y K, Liu B, Acharya J, Shirodkar S N, Luo J, Yan A, Charles D, Waghmare U V, Dravid V P and Rao C N R 2013 *ACS Nano* **7** 4879

[11] Lauritsen J V, Kibsgaard J, Helveg S, Topsoe H, Clausen B S, Laegsgaard E and Besenbacher F 2007 *Nat. Nanotechnol.* **2** 53

[12] Jaramillo T F, Jørgensen K P, Bonde J, Nielsen J H, Horch S and Chorkendorff I 2007 *Science* **317** 100

[13] Eng A Y S, Ambrosi A, Sofer Z, Simek P and Pumera M 2014 *ACS Nano* **8** 12185

[14] Xie J, Zhang J, Li S, Grote F, Zhang X, Zhang H, Wang R, Lei Y, Pan B and Xie Y 2013 *J. Am. Chem. Soc.* **135** 17881

[15] Liu N, Kim P, Kim J H, Ye J H, Kim S and Lee C J 2014 *ACS Nano* **8** 6902

[16] Faber M S and Jin S 2014 *Energy Environ. Sci.* **7** 3519

[17] Chettri M, Gupta U, Yadgarov L, Rosentveig R, Tenne R and Rao C N R 2015 *Dalton Trans.* **44** 16399

[18] Merki D, Vrubel H, Rovelli L, Fierro S and Hu X 2012 *Chem. Sci.* **3** 2515

[19] Kiran V, Mukherjee D, Jenjeti R N and Sampath S 2014 *Nanoscale* **6** 12856

[20] Xu C, Peng S, Tan C, Ang H, Tan H, Zhang H and Yan Q 2014 *J. Mater. Chem. A* **2** 5597

[21] Zhang X, Meng F, Mao S, Ding Q, Shearer M J, Faber M S, Chen J, Hamers R J and Jin S 2015 *Energy Environ. Sci.* **8** 862

[22] Cong C, Shang J, Wu X, Cao B, Peimyoo N, Qiu C, Sun L and Yu T 2014 *Adv. Opt. Mater.* **2** 131

[23] Berkdemir A, Gutierrez H R, Botello-Mendez A R, Perea-Lopez N, Elias A L, Chia C-I, Wang B, Crespi V H, Lopez-Urias F, Charlier J-C, Terrones H and Terrones M 2013 *Sci. Rep.* **3** 1755

[24] Elias A L, Perea-Lopez N, Castro-Beltran A, Berkdemir A, Lv R, Feng S, Long A D, Hayashi T, Kim Y A, Endo M, Gutierrez H R, Pradhan N R, Balicas L, Mallouk T E, Lopez-Urias F, Terrones H and Terrones M 2013 *ACS Nano* **7** 5235

[25] Nakamura K, Fujitsuka M and Kitajima M 1990 *Phys. Rev. B* **41** 12260

[26] Gouadec G and Colomban P 2007 *Prog. Cryst. Growth Charact. Mater.* **53** 1

[27] Voiry D, Salehi M, Silva R, Fujita T, Chen M, Asefa T, Shenoy V B, Eda G and Chhowalla M 2013 *Nano Lett.* **13** 222

[28] Somorjai G A 2002 *Topics Catal.* **18** 158

[29] Wang F, Li J, Wang F, Shifa T K A, Cheng Z, Wang Z, Xu K, Zhan X, Wang Q, Huang Y, Jiang C and He J 2015 *Adv. Funct. Mater.* **25** 6077

[30] Xu K, Wang F, Wang Z, Zhan X, Wang Q, Cheng Z, Safdar M and He J 2014 *ACS Nano* **8** 8468

[31] Fu Q, Yang L, Wang W, Han A, Huang J, Du P, Fan Z, Zhang J and Xiang B 2015 *Adv. Mater.* **27** 4732